

# An effective preparation method of composite photocatalysts for hydrogen evolution using an organic photosensitizer and metal particles assembled on alumina-silica

メタデータ	言語: English 出版者: Elsevier 公開日: 2018-12-28 キーワード (Ja): 光触媒, 水素製造 キーワード (En): Photocatalyst, Hydrogen production, Preparation method, Organic photosensitizer 作成者: 山田, 裕介, 田所, 秀之, 福住, 俊一 メールアドレス: 所属: Osaka City University, Japan Science and Technology Agency, Japan Science and Technology Agency, Ewha Womans University
URL	<a href="https://ocu-omu.repo.nii.ac.jp/records/2019703">https://ocu-omu.repo.nii.ac.jp/records/2019703</a>

# An effective preparation method of composite photocatalysts for hydrogen evolution using an organic photosensitizer and metal particles assembled on alumina-silica

Yusuke Yamada, Hideyuki Tadokoro and Shunichi Fukuzumi

<b>Citation</b>	Catalysis Today, 278(2): 303-311
<b>Issue Date</b>	2016-12-1
<b>Type</b>	Journal Article
<b>Textversion</b>	author
<b>Supplementary data</b>	Supplementary data is available at <a href="https://doi.org/10.1016/j.cattod.2016.01.018">https://doi.org/10.1016/j.cattod.2016.01.018</a> .
<b>Rights</b>	©2016 Elsevier B.V. This manuscript version is made available under the CC-BY-NC-ND 4.0 License. <a href="http://creativecommons.org/licenses/by-nc-nd/4.0/">http://creativecommons.org/licenses/by-nc-nd/4.0/</a> . This is the accepted manuscript version. The article has been published in final form at <a href="https://doi.org/10.1016/j.cattod.2016.01.018">https://doi.org/10.1016/j.cattod.2016.01.018</a> .
<b>DOI</b>	10.1016/j.cattod.2016.01.018

Self-Archiving by Author(s)  
Placed on: Osaka City University

**An Effective Preparation Method of Composite Photocatalysts for Hydrogen Evolution  
Using an Organic Photosensitizer and Metal Particles Assembled on Alumina-Silica**

Yusuke Yamada<sup>a,\*</sup>, Hideyuki Tadokoro<sup>b</sup>, and Shunichi Fukuzumi<sup>c,d,\*</sup>

<sup>a</sup>Department of Applied Chemistry and Bioengineering, Graduate School of Engineering, Osaka City University, 3-3-138 Sugimoto, Sumiyoshi-ku, Osaka 558-8585, Japan

<sup>b</sup>Department of Material and Life Science, Graduate School of Engineering, Osaka University, ALCA and SENTAN, Japan Science and Technology Agency (JST), Suita, Osaka 565-0871, Japan

<sup>c</sup>Faculty of Science and Engineering, Meijo University, ALCA and SENTAN, Japan Science and Technology Agency (JST), Nagoya, Aichi 468-0073, Japan

<sup>d</sup>Department of Chemistry and Nano Science, Ewha Womans University, Seoul 120-750, Korea

\* To whom correspondence should be addressed.

E-mail: ymd@a-chem.eng.osaka-cu.ac.jp; fukuzumi@chem.eng.osaka-u.ac.jp

## Abstract

Composite catalysts for photocatalytic hydrogen ( $H_2$ ) evolution were prepared by loading an organic electron donor-acceptor linked dyad [2-phenyl-4-(1-naphthyl)quinolinium ion,  $QuPh^+-NA$ ] as an organic photosensitizer and Pt or Cu particles as  $H_2$ -evolution catalysts on alumina-silica. The composite catalysts loading Pt particles were prepared by two different methods; first, Pt particles were deposited by reduction of  $PtCl_6^{2-}$  owing to photocatalysis of  $QuPh^+-NA$  supported on alumina-silica (PD method), and second, alumina-silica was impregnated with the  $PtCl_6^{2-}$  and calcined, and then  $QuPh^+-NA$  was loaded on the Pt/alumina-silica by a cation exchange method (IMP method). When a composite catalyst was prepared by the IMP method, a high Pt-loading amount of 4.2 wt% was necessary to achieve the highest  $H_2$ -evolution rate of  $0.27 \mu mol h^{-1}$ . On the other hand, a composite catalyst prepared by the PD method exhibited three times faster  $H_2$  evolution ( $0.83 \mu mol h^{-1}$ ) even though the loading amount of Pt was as low as 0.4 wt%. The activity of composite catalysts prepared by the PD method highly depends on the electric charges of precursors for Pt particles. A composite catalyst prepared with positively charged  $Pt(NH_3)_4^{2+}$  as a precursor of Pt particles exhibited low catalytic activity with the  $H_2$ -evolution rate of  $0.10 \mu mol h^{-1}$ , which is significantly lower than the rate ( $0.27 \mu mol h^{-1}$ ) for the composite catalyst prepared with  $PtCl_6^{2-}$ . However, such precursor-dependence was not observed for composite catalysts employing Cu particles as an  $H_2$ -evolution catalyst, because the Cu precursors are more labile than the Pt precursors in a reaction solution. The electrostatic interaction between the precursors of metal particles and negatively charged surfaces of alumina-silica should be taken into account to construct efficient  $H_2$ -evolution catalysts.

**Keywords:** Photocatalyst; Hydrogen production; Preparation method; Organic photosensitizer

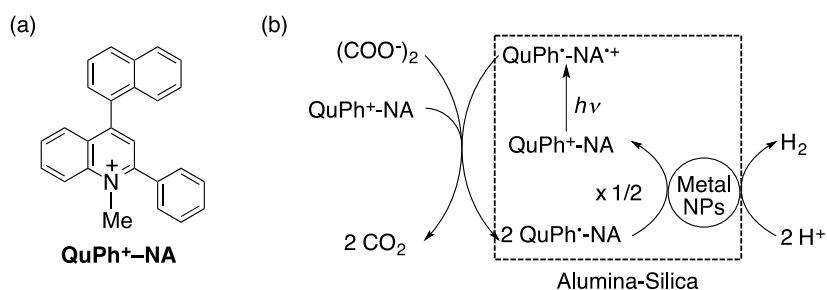
## 1. Introduction

Utilization of solar energy to produce high-energy compounds such as hydrogen ( $H_2$ ) attracts much attention to realize environmentally benign and sustainable society [1-5]. Two typical photocatalytic  $H_2$ -evolution systems have been extensively studied. One is a system using a semiconductor photocatalyst, which can split water to  $H_2$  and  $O_2$  under UV irradiation [6-9]. The fine-tuning of the bandgap of a metal-oxide semiconductor photocatalyst by doping nitrogen or sulfur has enabled to utilize visible light for the photocatalytic  $H_2$  production from water [10-11]. However, the quantum efficiency under visible light has remained low for any practical applications. The other system for photocatalytic  $H_2$  production utilizes metal complexes or organic molecules as photosensitizers together with a water reduction catalyst in homogeneous systems for efficient utilization of visible light [12-23]. In these systems sacrificial electron donors are required for the  $H_2$  evolution. To replace sacrificial electron donors to water as an electron donor, combination of the  $H_2$ -evolution systems with water oxidation catalysts is necessary [24-33]. However, simple combination of water oxidation catalysts with water reduction catalysts in a solution results in the reversed flow of electrons from the reduced water reduction catalysts to the oxidized water oxidation catalysts. The undesired back electron transfer can be avoided by rational arrangement of photosensitizers and catalysts for water oxidation and reduction on a suitable support, where the movement of each component can be suppressed. Development of procedure to prepare composite catalysts having rational arrangement of each component on the support is crucial to construct  $H_2$ -evolution systems utilizing visible light.

Before constructing a fully assembled catalyst, we have combined an organic photosensitizer [2-phenyl-4-(1-naphthyl)quinolinium ion,  $QuPh^+-NA$ ] and a water reduction catalyst (Pt, Cu, etc) on alumina-silica, which successfully exhibited photocatalytic activity for the  $H_2$  evolution

employing oxalate as an electron donor [34]. QuPh<sup>+</sup>-NA is an electron donor-acceptor linked dyad which possesses not only an extremely long lifetime of an electron-transfer state but also strong oxidizing and reducing abilities under photoirradiation [35]. The chemical structure of QuPh<sup>+</sup>-NA used in this study and the overall photocatalytic cycle for H<sub>2</sub> evolution are depicted in Scheme 1 [36-42]. The catalytic cycle starts from photoexcitation of QuPh<sup>+</sup>-NA in which

**Scheme 1.** (a) Structure of QuPh<sup>+</sup>-NA and (b) the overall photocatalytic cycle for H<sub>2</sub> evolution on a composite catalyst using QuPh<sup>+</sup>-NA and metal nanoparticles on alumina-silica



electron transfer from the NA moiety to the singlet excited state of the QuPh<sup>+</sup> moiety occurs to produce the electron-transfer state (QuPh<sup>\*</sup>-NA<sup>+</sup>). Then, electron transfer from oxalate to QuPh<sup>\*</sup>-NA<sup>+</sup> occurs to produce CO<sub>2</sub> and CO<sub>2</sub><sup>•-</sup> and QuPh<sup>\*</sup>-NA. CO<sub>2</sub><sup>•-</sup> can transfer an electron to QuPh<sup>+</sup>-NA to produce CO<sub>2</sub> and QuPh<sup>\*</sup>-NA. Two equivalents of QuPh<sup>\*</sup>-NA thus produced can inject two electrons to metal nanoparticles to produce H<sub>2</sub> by reduction of two protons. In our previous work, combined catalysts were successfully prepared by the following two-step route (**PD** method): QuPh<sup>+</sup>-NA was first loaded on alumina-silica (QuPh<sup>+</sup>-NA@Al<sub>2</sub>O<sub>3</sub>-SiO<sub>2</sub>) by the cation exchange method and then, Pt or Cu particles were supported on the QuPh<sup>+</sup>-NA@Al<sub>2</sub>O<sub>3</sub>-SiO<sub>2</sub> by the reduction of PtCl<sub>6</sub><sup>2-</sup> or CuCl<sub>2</sub> *in situ* with photogenerated QuPh<sup>\*</sup>-NA [34]. However, preparation conditions to achieve highly active composite catalysts have yet to be clarified in terms of choices of precursors, and nanostructures and morphologies of silica-alumina supports, etc.

We report herein the effect of preparation conditions of the catalysts composed of alumina-silica loading QuPh<sup>+</sup>-NA and Pt particles on their catalysis for photocatalytic H<sub>2</sub> evolution using oxalate as a sacrificial electron donor. Other than the **PD** method, the impregnation method (**IMP** method), in which alumina-silica was impregnated with Pt and then loading QuPh<sup>+</sup>-NA by the cation-exchange method, was examined to construct a composite catalyst. Also, various types of Pt complexes and Pt salts were examined as precursors of Pt particles for the **PD** method. Additionally, nanostructures and morphologies of alumina-silica supports were optimized for further improvement in the photocatalytic reactivity. Suitable preparation conditions were also investigated for a composite catalyst employing Cu particles, which has been less studied as an H<sub>2</sub> evolution catalyst.

## 2. Experimental section

### 2.1 Catalyst preparation

All chemicals were obtained from chemical companies and used without further purification. K<sub>2</sub>Pt<sup>IV</sup>Cl<sub>6</sub>, Pt<sup>II</sup>(NH<sub>3</sub>)<sub>4</sub>Cl<sub>2</sub>, K<sub>2</sub>Cu<sup>II</sup>Cl<sub>4</sub>·2H<sub>2</sub>O, Ru<sup>III</sup>Cl<sub>3</sub>, Co<sup>II</sup>(NO<sub>3</sub>)<sub>2</sub>, Fe<sup>II</sup>SO<sub>4</sub>·7H<sub>2</sub>O, cetyltrimethylammonium bromide (CTAB), sodium aluminate, acetic acid, hydrochloric acid and sodium hydroxide were obtained from Wako Pure Chemical Industries. K<sub>2</sub>Pt<sup>II</sup>Cl<sub>4</sub> was purchased from Sigma-Aldrich. An aqueous solution of ammonia (28%) and  $\beta$ -nicotinamide adenine dinucleotide disodium salt (reduced form) (NADH) were obtained from Tokyo Chemical Industry. Tetraethyl orthosilicate (TEOS) was delivered by Shin-Etsu Chemical. 2-Phenyl-4-(1-naphthyl)quinolinium (QuPh<sup>+</sup>-NA) perchlorate was synthesized by a literature method [35]. Purified water was provided by a Millipore MilliQ UV-3 water purification system where the electronic conductance was 18.2 M $\Omega$  cm. Spherical Al-MCM-41 (sAlMCM-41), spherical Al<sub>2</sub>O<sub>3</sub>-SiO<sub>2</sub> (sAl<sub>2</sub>O<sub>3</sub>-SiO<sub>2</sub>) and unshape-controlled Al<sub>2</sub>O<sub>3</sub>-SiO<sub>2</sub> (uAl<sub>2</sub>O<sub>3</sub>-SiO<sub>2</sub>) were prepared by

literature methods [39]. *cis*-[Pt<sub>2</sub>(NH<sub>3</sub>)<sub>2</sub>(μ-C<sub>2</sub>H<sub>4</sub>NO)<sub>2</sub>](ClO<sub>4</sub>)<sub>2</sub>, [Cu(bpy)<sub>2</sub>](NO<sub>3</sub>)<sub>2</sub>·0.75H<sub>2</sub>O and [Cu(MeObpy)<sub>2</sub>](NO<sub>3</sub>)<sub>2</sub> were also synthesized by literature methods [43].

Unshape-controlled AIMCM-41 (uAIMCM-41) was prepared by the following procedure. To an aqueous solution (1.0 L) containing NaOH (8.4 g, 0.21 mol) and CTAB (18.4 g, 44.4 mmol) was added dropwise of TEOS (87.5 g, 418 mmol) with vigorous stirring for 1 h at 35 °C. The solution was further stirred for 30 min at the temperature. Then, an aqueous solution (100 mL) of sodium aluminate (0.48 g, 7.9 mmol) was slowly added to the solution and stirred for 4 h at room temperature. The obtained white precipitate was filtered, washed with water and dried at 60 °C. The precipitate was calcined at 500 °C for 6 h with a ramp rate of 1 °C min<sup>-1</sup>.

Unshape-controlled Al<sub>2</sub>O<sub>3</sub>-SiO<sub>2</sub> was prepared by the surface alumination of unshaped silica powder. Silica powder (10-20 nm, 3.0 g, 50 mmol) was suspended in an aqueous solution (150 mL) of sodium aluminate (0.19 mg, 3.1 mmol) with magnetic stirring at room temperature for 24 h. The obtained powder was collected by centrifugation, washed with water, and dried at 60 °C. The obtained white powder was calcined at 550 °C for 5 h with a ramp rate of 1 °C min<sup>-1</sup>.

sAIMCM-41 loading Pt (Pt/sAIMCM-41) was prepared by an impregnation method. sAIMCM-41 (500 mg) was immersed in an ethanol solution (1.0 mL) containing a calculated amount of K<sub>2</sub>PtCl<sub>6</sub> on an ultrasonicator for 30 min at room temperature. The powder was dried at 60 °C in air and calcined at 500 °C for 4 h with a ramp rate of 2 °C min<sup>-1</sup>. The loading amount of Pt was determined by X-ray fluorescence measurements performed with a Rigaku ZSX-100e.

Alumina-silica loading QuPh<sup>+</sup>-NA was prepared by the cation-exchange method. An acetonitrile solution (10 mL) of QuPh<sup>+</sup>-NA (6.0 mM or 2.0 mM) was slowly added to an aqueous suspension (10 mL) containing alumina-silica (200 mg) with gentle magnetic stirring. After keeping for a certain time at room temperature, the supernatant was removed and dried at

60 °C. The amount of QuPh<sup>+</sup>-NA was determined by the decrease of absorbance at 333 nm originated from QuPh<sup>+</sup>-NA ion. The same procedure was applied for loading QuPh<sup>+</sup>-NA on Pt/sAlMCM to achieve a composite catalyst (**IMP** method). Composite catalysts prepared by the **PD** method were obtained by photoirradiation ( $\lambda > 340$  nm) of suspension containing alumina-silica loading QuPh<sup>+</sup>-NA, K<sub>2</sub>PtCl<sub>6</sub> and oxalic acid. The obtained catalysts were used for the catalysis measurements without isolation.

## 2.2. Catalyst characterization

Transmission electron microscopy (TEM) was used for the determination of the sizes and shapes of catalysts. Bright field images were obtained by a JEOL JEM-2100 that has a thermal field emission gun with an accelerating voltage of 200 kV. The observed samples were prepared by dropping a suspension of catalysts, allowing the solvent to evaporate and then scooped up with an amorphous carbon supporting film. Nitrogen adsorption-desorption at 77 K was performed with a Belsorp-mini (BEL Japan, Inc.) within a relative pressure range from 0.01 to 101.3 kPa. A sample mass of ~100 mg was used for adsorption analysis after pretreatment at 120 °C for 1 h under vacuum conditions and kept in N<sub>2</sub> atmosphere until N<sub>2</sub>-adsorption measurements. The samples were exposed to a mixed gas of He and N<sub>2</sub> with a programmed ratio and adsorbed amount of N<sub>2</sub> was calculated from the change of pressure in a cell after reaching the equilibrium. The surface area of each catalyst was determined by the Brunauer-Emmett-Teller (BET) method for multiple N<sub>2</sub> adsorption amounts under the conditions of partial pressure less than 0.3. The sizes of mesopores of alumina-silica (AlMCM-41 and sAlMCM-41) were determined by the MP method. Powder X-ray diffraction patterns were recorded by a Rigaku Miniflex 600. Incident X-ray radiation was produced by a Cu X-ray tube, operating at 40 kV and 15 mA with Cu *K* $\alpha$  radiation of 1.54 Å. The scanning rate was 2° min<sup>-1</sup> from 5° to 80° in  $2\theta$ .

### 2.3. Catalysis measurements

A typical procedure for photocatalytic H<sub>2</sub> evolution is as follows: an aqueous phthalate buffer (50 mM, pH 4.5, 2.0 mL) containing QuPh<sup>+</sup>-NA@sAlMCM-41 composite (QuPh<sup>+</sup>-NA: 0.22 mM), and K<sub>2</sub>PtCl<sub>6</sub> (0.027 mM) was flushed with N<sub>2</sub> gas in dark. The suspension was then photoirradiated for a certain time with a xenon lamp (Ushio Optical, Model X SX-UID 500X AMQ) through a color filter glass (Asahi Techno Glass L39) transmitting  $\lambda > 340$  nm at room temperature. After 1 min stirring in the dark, gas in a headspace was analyzed by Shimadzu GC-14B gas chromatography (detector: TCD, column temperature: 50 °C, column: active carbon with the particle size 60-80 mesh, carrier gas: N<sub>2</sub> gas) to quantify evolved H<sub>2</sub>.

## 3. Results and discussion

### 3.1. Catalysis of composite catalysts loading Pt by an impregnation and a photodeposition method for photocatalytic H<sub>2</sub> evolution

Composite catalysts loading an organic photosensitizer [2-phenyl-4-(1-naphthyl)quinolinium ion, QuPh<sup>+</sup>-NA] and an H<sub>2</sub>-evolution catalyst, Pt particles, on alumina-silica for photocatalytic H<sub>2</sub>-evolution were prepared by two different methods: an **IMP** method and a **PD** method. In the **IMP** method, composite catalysts were prepared by impregnation of alumina-silica with an aqueous solution of K<sub>2</sub>PtCl<sub>6</sub> as a precursor, followed by calcination, and then QuPh<sup>+</sup>-NA was loaded by the cation-exchange method on the calcined alumina-silica loading Pt. In the **PD** method, QuPh<sup>+</sup>-NA was supported on alumina-silica (QuPh<sup>+</sup>-NA@alumina-silica) by the cation-exchange method and then, the QuPh<sup>+</sup>-NA@alumina-silica was suspended in an aqueous phthalate buffer (pH 4.5) containing K<sub>2</sub>PtCl<sub>6</sub> and oxalic acid. Pt particles were deposited on the QuPh<sup>+</sup>-NA@alumina-silica by photoirradiation of the suspension. Pt particles deposited on

QuPh<sup>+</sup>-NA@alumina-silica was confirmed by the TEM images shown in Fig. 1, in which the sizes of the Pt particles were smaller than 1 nm. The concentration of Pt deposited on

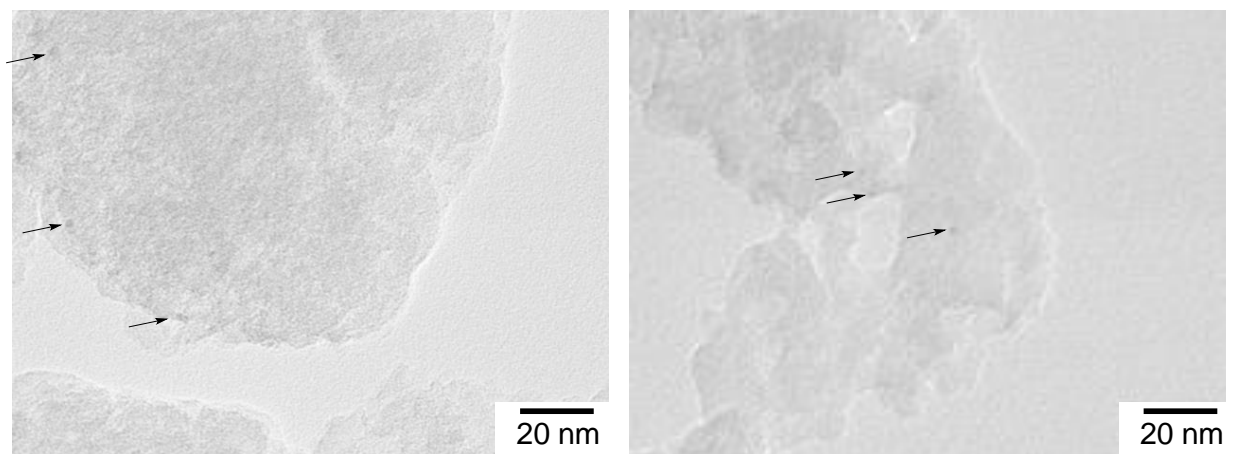


**Fig. 1.** TEM images of QuPh<sup>+</sup>-NA@sAIMCM-41 loading Pt particles by the photodeposition method. Relatively large Pt nanoparticles are indicated by the arrows.

QuPh<sup>+</sup>-NA/sAIMCM-41 after the photocatalytic reaction was determined to be 0.3 ( $\pm$  0.1) wt% in the solution containing 0.027 mM K<sub>2</sub>PtCl<sub>6</sub> by XRF measurements, where the maximum concentration of Pt is 0.21 wt%. Thus, almost all Pt ions were converted to Pt particles.

Photocatalytic H<sub>2</sub> evolution was performed by photoirradiation ( $\lambda > 340$  nm) of an aqueous phthalate buffer (50 mM, pH 4.5, 2.0 mL) containing oxalate (50 mM) and the catalysts loading various amounts of Pt ([QuPh<sup>+</sup>-NA]: 0.22 mM, [Pt]: 0.013 – 0.55 mM) prepared by the **IMP** method. The H<sub>2</sub>-evolution rate increased in proportion to the loading amount of Pt up to 2.1 wt% ([Pt]: 0.27 mM in the reaction solution) as shown in Fig. 2a. No further increase in the H<sub>2</sub>-evolution rate was observed by increasing the loading amount of Pt to 4.2 wt% ([Pt]: 0.55 mM). The saturation behavior against the loading amount of Pt resulted from enough high surface density of Pt particles at 2.1 wt% to be interacted with all the QuPh<sup>+</sup>-NA loaded on the alumina-silica.

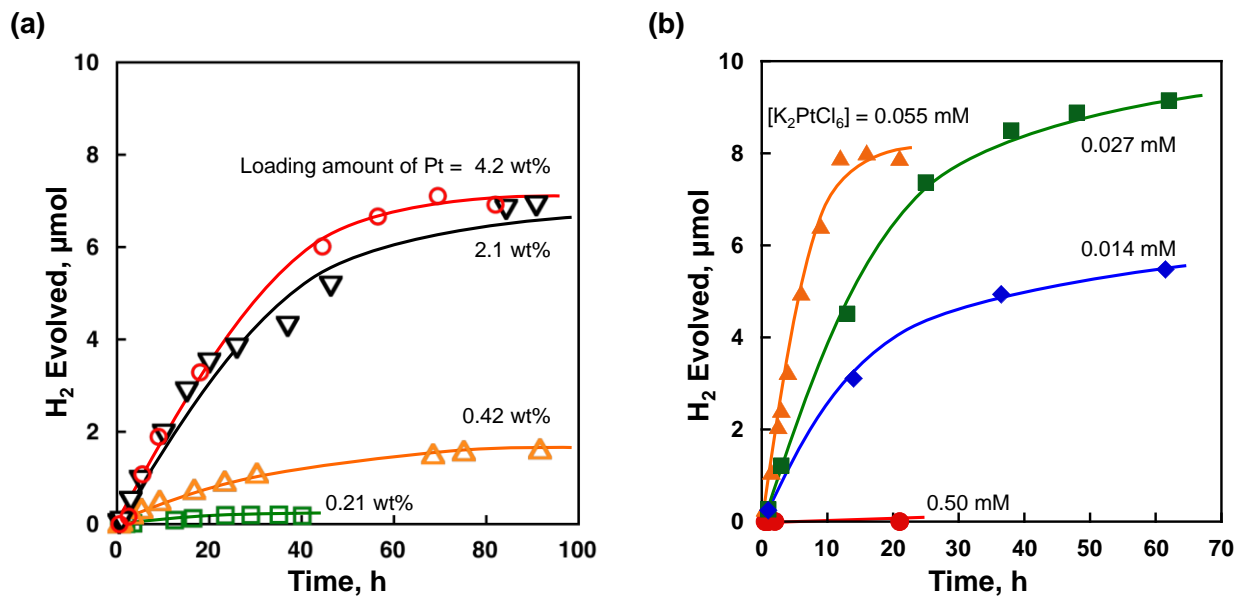


**Fig. 2.** Time courses of the photocatalytic H<sub>2</sub> evolution performed by photoirradiation ( $\lambda > 340$  nm) of a deaerated phthalate buffer (pH 4.5, 2.0 mL) containing (COONa)<sub>2</sub> (50 mM) and various Pt-loaded QuPh<sup>+</sup>-NA@alumina-silica (sAlMCM-41) catalysts (~3.0 mg, [QuPh<sup>+</sup>-NA]: 0.22 mM) prepared by the impregnation (**IMP**) method and the photodeposition (**PD**) method. (a) **IMP** method: Pt loadings [0.21 wt% (green open square), 0.42 wt% (orange open triangle), 2.1 wt% (black open inverted triangle) and 4.2 wt% (red open circle)] and (b) **PD** method: the concentrations of PtCl<sub>6</sub><sup>2-</sup> in solutions [0.014 mM (blue diamond), 0.027 mM (green square), 0.055 mM (orange triangle) and 0.50 mM (red circle)].

Photocatalytic activity of the composite catalysts prepared by the **PD** method was also evaluated by the photoirradiation of an aqueous phthalate buffer containing QuPh<sup>+</sup>-NA/alumina-silica, (COONa)<sub>2</sub> and K<sub>2</sub>PtCl<sub>6</sub> with various concentrations (0.018 – 0.50 mM) (Fig. 2b). The composite catalysts formed *in situ* under reaction conditions and used without separation from the suspension. The H<sub>2</sub>-evolution rate was increased to 0.83 μmol h<sup>-1</sup> by increasing the concentration of K<sub>2</sub>PtCl<sub>6</sub> up to 0.055 mM, which is 10 times larger than that (0.07 μmol h<sup>-1</sup>) for a composite catalyst loading the same amount of Pt by the **IMP** method (0.42 wt%). Turnover numbers of Pt for H<sub>2</sub> evolution were 14 and 73 for composite catalysts loading Pt (0.42 wt%) by the **IMP** and **PD** methods, respectively. Thus, the **PD** method is the more suitable method to

achieve an efficient photocatalytic H<sub>2</sub>-evolution system than the **IMP** method with a small amount of Pt.

### 3.2. Precursor effect on H<sub>2</sub>-evolution catalysis of composite catalysts prepared by the PD method

Catalytic activity of composite catalysts loading Pt by the photodeposition method depends on Pt precursors. Composite catalysts were *in situ* prepared by the **PD** method in an aqueous buffer containing oxalate, QuPh<sup>+</sup>-NA@sAIMCM-41 and various Pt precursors ([Pt]: 0.027 mM). Time courses of H<sub>2</sub> evolution for the reaction systems using various Pt precursors are indicated in Fig. 3. When anionic PtCl<sub>6</sub><sup>2-</sup> and PtCl<sub>4</sub><sup>2-</sup> were used as precursors, the initial H<sub>2</sub>-evolution rates (5 h) were 0.31 and 0.40 μmol h<sup>-1</sup>, respectively. Although the concentration of Pt is the

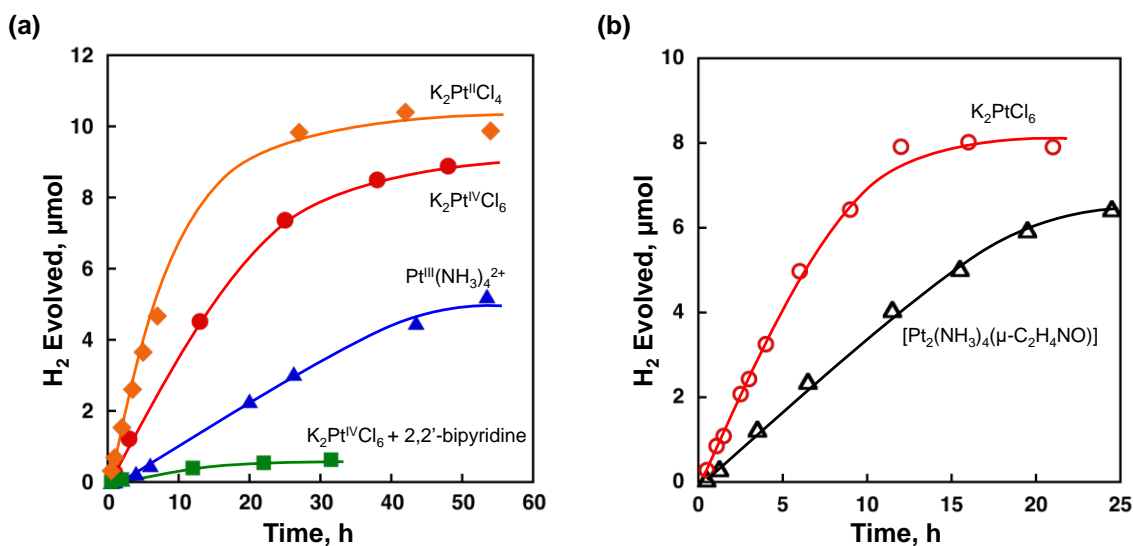


**Fig. 3.** Time courses of hydrogen evolution by photoirradiation ( $\lambda > 340$  nm) of an aqueous buffer (2.0 mL) containing oxalate (50 mM), QuPh<sup>+</sup>-NA@sAIMCM-41 (5.0 mg, [QuPh<sup>+</sup>-NA]: 0.22 mM) and various Pt precursors. Pt precursors were (a) PtCl<sub>6</sub><sup>2-</sup> (red circle), PtCl<sub>4</sub><sup>2-</sup> (orange diamond), Pt(NH<sub>3</sub>)<sub>4</sub><sup>2+</sup> (blue triangle) and PtCl<sub>6</sub><sup>2-</sup> together with 2,2'-bipyridine (0.081 mM) (green square); [Pt]= 0.027 mM and (b) PtCl<sub>6</sub><sup>2-</sup> (red open circle) and *cis*-[Pt<sub>2</sub>(NH<sub>3</sub>)<sub>4</sub>(μ-C<sub>2</sub>H<sub>4</sub>NO)] (black open triangle); [Pt]= 0.055 mM.

same, slower H<sub>2</sub> evolution (0.11 μmol h<sup>-1</sup>) was observed for the reaction systems using positively charged Pt(NH<sub>3</sub>)<sub>4</sub><sup>2+</sup> as a precursor, suggesting that the electric charges of precursors should be taken into consideration to construct an efficient photocatalytic system. Positively-charged Pt(NH<sub>3</sub>)<sub>4</sub><sup>2+</sup> has attractive interaction with negatively charged surfaces of alumina-silica where it may be trapped far from the loaded QuPh<sup>+</sup>-NA molecules. Thus, the anionic precursors, i.e. PtCl<sub>6</sub><sup>2-</sup> and PtCl<sub>4</sub><sup>2-</sup>, which can interact with positively charged QuPh<sup>+</sup>-NA but not with the negatively charged surfaces of alumina-silica, are suitable for construction of an efficient photocatalytic H<sub>2</sub>-evolution system. When 2,2'-bipyridine (bpy) was added to the reaction solution containing PtCl<sub>6</sub><sup>2-</sup>, only negligible amount of H<sub>2</sub> was evolved probably due to the coordination of chelating bpy ligand to Pt<sup>IV</sup> ion strongly preventing the deposition of Pt particles. A significant amount of H<sub>2</sub> evolution was observed for a reaction solution containing *cis*-[Pt<sub>2</sub>(NH<sub>3</sub>)<sub>4</sub>(μ-CH<sub>2</sub>NO)<sub>2</sub>], which has been reported to act as a homogeneous catalyst for H<sub>2</sub> evolution (Fig. 3b) [43]. However, the H<sub>2</sub> evolution from the reaction system using *cis*-[Pt<sub>2</sub>(NH<sub>3</sub>)<sub>4</sub>(μ-CH<sub>2</sub>NO)<sub>2</sub>] was slower than that using PtCl<sub>6</sub><sup>2-</sup>. Thus, the deposition of Pt particles in the close vicinity of QuPh<sup>+</sup>-NA is important to achieve efficient H<sub>2</sub> evolution.

The effect of concentrations of oxalic acid on H<sub>2</sub>-evolution rates was examined in the photocatalytic H<sub>2</sub> evolution employing catalysts prepared by the **PD** method with K<sub>2</sub>PtCl<sub>6</sub> (Fig. 4). According to the p*K*<sub>a1</sub> (1.2) and p*K*<sub>a2</sub> (4.3) values of oxalic acid, dianion species of oxalic acid was mainly formed in the buffer with pH 4.5 [44]. The initial H<sub>2</sub>-evolution rate increased in proportion to the concentration of oxalate dianion up to 25 mM. No further increase in the H<sub>2</sub>-evolution rate was observed even at a concentration of oxalic acid higher than 25 mM, suggesting that the oxalate concentration of 25 mM is enough high to fully reduce photoexcited QuPh<sup>+</sup>-NA (QuPh<sup>•</sup>-NA<sup>•+</sup>) under the current reaction conditions.

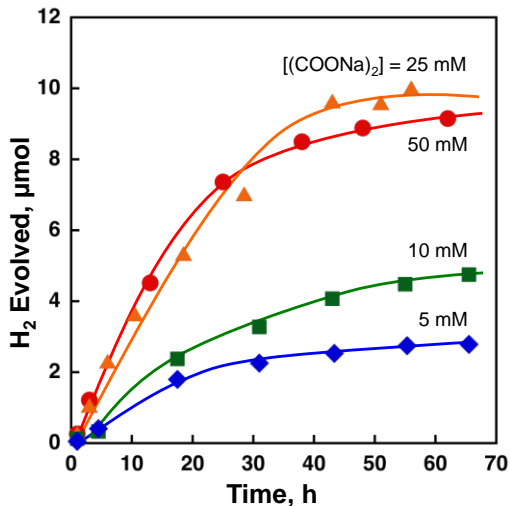


**Fig. 4.** Time courses of the photocatalytic H<sub>2</sub> evolution in various concentrations of (COONa)<sub>2</sub> (5.0 mM, blue diamond; 10 mM, green square; 25 mM, orange triangle; 50 mM, red circle). H<sub>2</sub> evolution was performed under photoirradiation ( $\lambda > 340$  nm) of a deaerated phthalate buffer (pH 4.5, 2.0 mL) containing QuPh<sup>+</sup>-NA@sAlMCM41 (5.0 mg, [QuPh<sup>+</sup>-NA] = 0.22 mM) and (COONa)<sub>2</sub> (5.0 – 50 mM) with K<sub>2</sub>PtCl<sub>6</sub> (0.027 mM) at 298 K.

### 3.3. Effect of nanostructures and morphologies of alumina-silica supports

Nanostructures and morphologies of alumina-silica supports effect on the photocatalysis of composite catalysts for H<sub>2</sub> evolution. The supports were classified into the following four groups based on the morphology and porosity; spherical alumina-silica with mesopores (sAlMCM-41, Fig. 5a), unshape-controlled alumina-silica with mesopores (AlMCM-41, Fig. 5b), spherical alumina-silica without pores (sAl<sub>2</sub>O<sub>3</sub>-SiO<sub>2</sub>, Fig. 5c) and unshape-controlled alumina-silica without pores (Al<sub>2</sub>O<sub>3</sub>-SiO<sub>2</sub>, Fig. 5d). The surface areas and pore diameters of the supports were characterized by N<sub>2</sub> adsorption-desorption isotherms (Fig. 6). The isotherms obtained for sAlMCM-41 and AlMCM-41 were categorized to Type IV, which suggests mesoporous structures [45]. The pore diameters estimated by the MP method were about 1 nm for both samples. On the other hand, Type III isotherms obtained for both sAl<sub>2</sub>O<sub>3</sub>-SiO<sub>2</sub> and Al<sub>2</sub>O<sub>3</sub>-SiO<sub>2</sub>

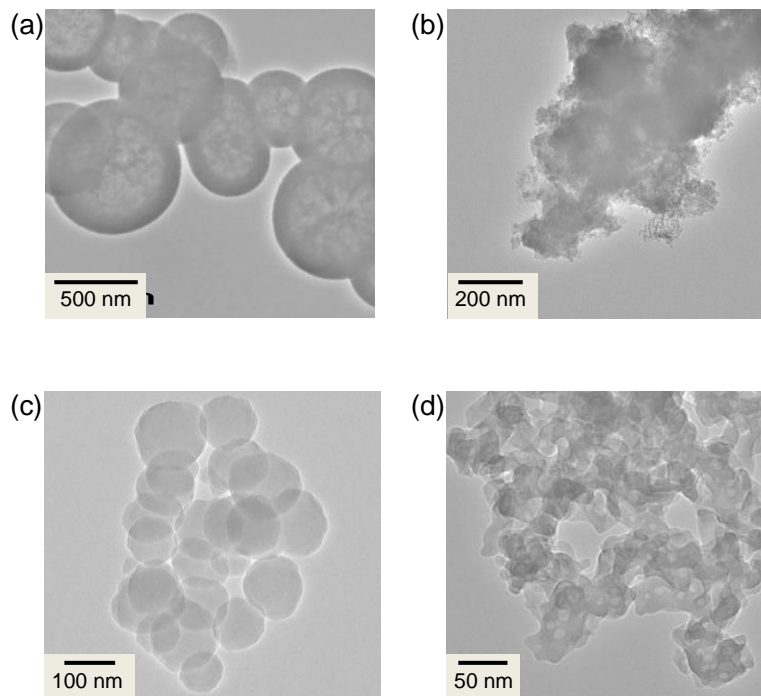


**Fig. 5.** TEM images of (a) sAIMCM-41, (b) AIMCM-41, (c) sAl<sub>2</sub>O<sub>3</sub>-SiO<sub>2</sub> NP and (d) Al<sub>2</sub>O<sub>3</sub>-SiO<sub>2</sub>.

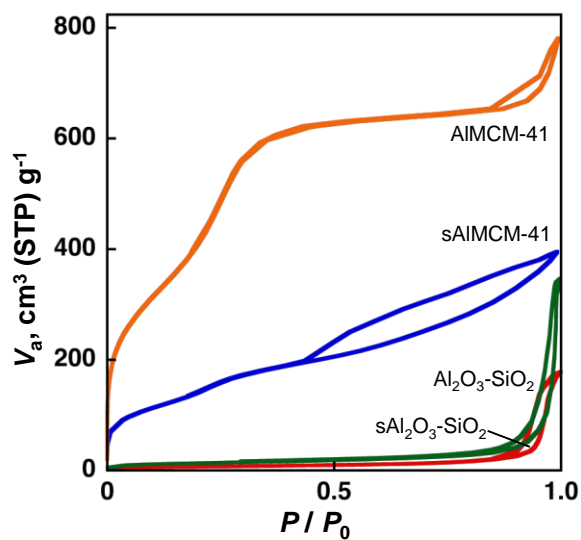


**Fig. 6.** Nitrogen adsorption-desorption isotherms of alumina-silica with various nanostructures and morphologies. [(a) sAIMCM-41 (blue), (b) AIMCM-41 (orange), (c) sAl<sub>2</sub>O<sub>3</sub>-SiO<sub>2</sub> (red) and (d) Al<sub>2</sub>O<sub>3</sub>-SiO<sub>2</sub> (green)]

assured non-porous structure [45]. Table 1 summarizes the surface areas, pore sizes and adsorbed amount of QuPh<sup>+</sup>-NA. The densities of QuPh<sup>+</sup>-NA on the surfaces of sAlMCM-41, AlMCM-41, sAl<sub>2</sub>O<sub>3</sub>-SiO<sub>2</sub> and Al<sub>2</sub>O<sub>3</sub>-SiO<sub>2</sub> were 0.17, 0.04, 0.80 and 0.79 molecules nm<sup>-2</sup>, respectively, suggesting that QuPh<sup>+</sup>-NA molecules are isolated. The lower densities obtained for mesoporous alumina-silica may suggest that QuPh<sup>+</sup>-NA cannot penetrate deeply inside mesopores.

**Table 1.** Specific surface area and pore diameter, morphology and amount of QuPh<sup>+</sup>-NA adsorbed on alumina-silica.

	Morphology	BET surface area (m <sup>2</sup> g <sup>-1</sup> )	Pore diameter <sup>[a]</sup> (nm)	Amount of QuPh <sup>+</sup> -NA <sup>[b]</sup> (mol g <sup>-1</sup> )
sAlMCM-41	Spherical	797	1.0	2.3 × 10 <sup>-4</sup>
AlMCM-41	Unshaped	1471	1.1	9.9 × 10 <sup>-5</sup>
sAl <sub>2</sub> O <sub>3</sub> -SiO <sub>2</sub>	Spherical	24		3.2 × 10 <sup>-5</sup>
Al <sub>2</sub> O <sub>3</sub> -SiO <sub>2</sub>	Unshaped	47		6.2 × 10 <sup>-5</sup>

[a] determined by the MP method using desorption branch of N<sub>2</sub>-isotherm at 77 K. [b] The loading amount of QuPh<sup>+</sup>-NA was calculated from decrease in absorbance at 333 nm characteristic of QuPh<sup>+</sup>-NA caused by the addition of alumina-silica to mother liquor.

Activity of the composite catalysts employing these four alumina-silica supports was examined for photocatalytic H<sub>2</sub> evolution in a phthalate buffer together with oxalate anion (50 mM) and Pt<sup>IV</sup>Cl<sub>6</sub><sup>2-</sup>. The amounts of used catalysts were normalized by the concentration of QuPh<sup>+</sup>-NA to be 0.22 mM. Fig. 7 shows the time courses of H<sub>2</sub> evolution from the reaction suspensions under photoirradiation. The fastest initial H<sub>2</sub> evolution (0.83 μmol h<sup>-1</sup>) was obtained for the composite catalyst using sAlMCM-41, however, the H<sub>2</sub> evolution was ceased after photoirradiation for 10 h. The composite catalyst employing AlMCM-41 as a support exhibited slower H<sub>2</sub> evolution (0.22 μmol h<sup>-1</sup>) with the amount less than 5 μmol. Composite catalyst using non-porous sAl<sub>2</sub>O<sub>3</sub>-SiO<sub>2</sub>

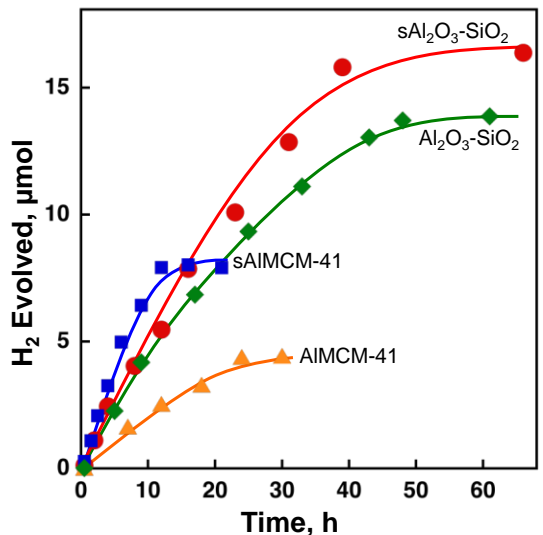


**Fig. 7.** Time courses of H<sub>2</sub> evolution under photoirradiation ( $\lambda > 340$  nm) of a deaerated mixed solution (2.0 mL) of a phthalate buffer (pH 4.5) containing K<sub>2</sub>PtCl<sub>6</sub> (0.055 mM), (COONa)<sub>2</sub> (50 mM) and QuPh<sup>+</sup>-NA@silica-alumina ([QuPh<sup>+</sup>-NA] = 0.22 mM; QuPh<sup>+</sup>-NA@sAIMCM-41, 5.0 mg, blue square; QuPh<sup>+</sup>-NA@AIMCM-41, 4.4 mg, orange triangle; QuPh<sup>+</sup>-NA@sAl<sub>2</sub>O<sub>3</sub>-SiO<sub>2</sub>, 13.6 mg, red circle; QuPh<sup>+</sup>-NA@Al<sub>2</sub>O<sub>3</sub>-SiO<sub>2</sub>, 7.1 mg, green diamond) at 298 K.

and Al<sub>2</sub>O<sub>3</sub>-SiO<sub>2</sub> as supports exhibited slower initial H<sub>2</sub> evolution compared with the catalyst using sAIMCM-41, however, higher durability was achieved as evidenced by the larger amount of H<sub>2</sub> evolution (16 and 13 μmol, respectively), which are more than double that of sAIMCM-41. These results suggest that the mesoporous silica-alumina is not a suitable support for constructing an active composite catalyst although reasons are unclear.

The effect of the loading amount of QuPh<sup>+</sup>-NA on a silica-alumina support was investigated. Photocatalytic H<sub>2</sub> evolution was performed by photoirradiation of a suspension containing K<sub>2</sub>PtCl<sub>6</sub>, (COONa)<sub>2</sub> and QuPh<sup>+</sup>-NA@Al<sub>2</sub>O<sub>3</sub>-SiO<sub>2</sub> (12.9 mg, [QuPh<sup>+</sup>-NA] = 0.22 mM), which was prepared by decreasing the loading amount of QuPh<sup>+</sup>-NA on Al<sub>2</sub>O<sub>3</sub>-SiO<sub>2</sub> from 64 to 34 μmol g<sup>-1</sup> as shown in Fig. 8. Although the concentrations of QuPh<sup>+</sup>-NA are the same in the reaction suspensions, reactivity of the Al<sub>2</sub>O<sub>3</sub>-SiO<sub>2</sub> loading a small amount of QuPh<sup>+</sup>-NA was

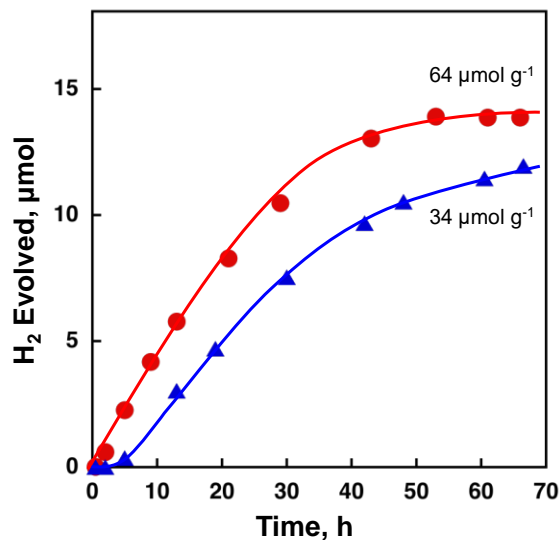


**Fig. 8.** Time courses of H<sub>2</sub> evolution under photoirradiation ( $\lambda > 340$  nm) of a deaerated phthalate buffer (pH 4.5, 2.0 mL) containing K<sub>2</sub>PtCl<sub>6</sub> (0.055 mM), (COONa)<sub>2</sub> (50 mM) and different amounts of QuPh<sup>+</sup>-NA@Al<sub>2</sub>O<sub>3</sub>-SiO<sub>2</sub> [7.1 mg ([QuPh<sup>+</sup>-NA] = 0.22 mM, 64  $\mu\text{mol g}^{-1}$ ), red circle; 12.9 mg ([QuPh<sup>+</sup>-NA] = 0.22 mM, 34  $\mu\text{mol g}^{-1}$ ), blue triangle].

slightly lower than that loading a large amount of QuPh<sup>+</sup>-NA. These results suggest that the catalysis of the composite catalyst may be improved by employing an optimum density of QuPh<sup>+</sup>-NA on the surfaces of alumina-silica.

### 3.4. Composite catalysts using Ru, Cu and Ni as H<sub>2</sub>-evolution catalysts

Other than Pt, nanoparticles of Ru, Fe and Ni have been reported to act as H<sub>2</sub>-evolution catalysts [36,38,46]. Thus, the photocatalytic H<sub>2</sub> evolution was conducted in an aqueous buffer (pH 4.5) containing QuPh<sup>+</sup>-NA@sAIMCM-41 and oxalic acid in the presence of Ru<sup>3+</sup>, Fe<sup>2+</sup>, Cu<sup>2+</sup>, Ni<sup>2+</sup> or Co<sup>2+</sup> ions in the form of RuCl<sub>3</sub>, FeSO<sub>4</sub>, Cu(NO<sub>3</sub>)<sub>2</sub>, Ni(NO<sub>3</sub>)<sub>2</sub> or Co(NO<sub>3</sub>)<sub>2</sub>, respectively. The time courses of H<sub>2</sub> evolution shown in Fig. 9 exhibited that the H<sub>2</sub>-evolution

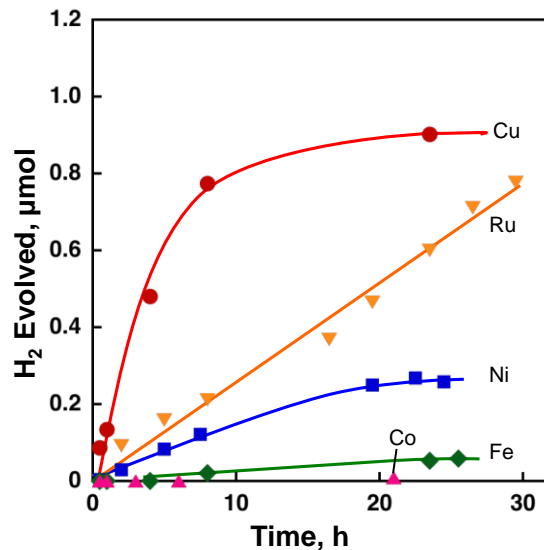


**Fig. 9.** Time courses of H<sub>2</sub> evolution under photoirradiation ( $\lambda > 340$  nm) of a deaerated phthalate buffer (pH 4.5) containing QuPh<sup>+</sup>-NA@sAIMCM-41 (5.0 mg, [QuPh<sup>+</sup>-NA] = 0.22 mM) and (COONa)<sub>2</sub> (50 mM) with various metal salts [0.055 mM; Cu(NO<sub>3</sub>)<sub>2</sub>, red circle; RuCl<sub>3</sub>, orange inverse triangle; Ni(NO<sub>3</sub>)<sub>2</sub>, blue square; FeSO<sub>4</sub>, green diamond; Co(NO<sub>3</sub>)<sub>2</sub>, pink triangle].

rate for the reaction system containing Cu<sup>2+</sup> ions was 0.11  $\mu\text{mol h}^{-1}$ , which is larger than those containing Ru<sup>3+</sup> (0.03  $\mu\text{mol h}^{-1}$ ), Ni<sup>2+</sup> (0.02  $\mu\text{mol h}^{-1}$ ), Fe<sup>2+</sup> (< 0.01  $\mu\text{mol h}^{-1}$ ) or Co<sup>2+</sup> (< 0.01  $\mu\text{mol h}^{-1}$ ) ions. Cu nanoparticles without a support has been reported to act as an inferior H<sub>2</sub>-evolution catalyst to Ru and Ni nanoparticles [38]. This is probably due to easy agglomeration properties of Cu nanoparticles, which can be suppressed by being loaded on sAIMCM-41. For example, the durability of Ru nanoparticles has been reported to be much improved by loading Ru nanoparticles on a silica support in comparison with that of unsupported Ru nanoparticles [39]. Thus, loading of Cu particles on a metal oxide support may also prevent agglomeration of Cu nanoparticles, leading to high catalytic activity.

The effect of concentration of Cu ions in the reaction suspension on the H<sub>2</sub> evolution was examined by changing the concentrations from 0.027 mM to 0.55 mM (Fig. 10). The fastest H<sub>2</sub>

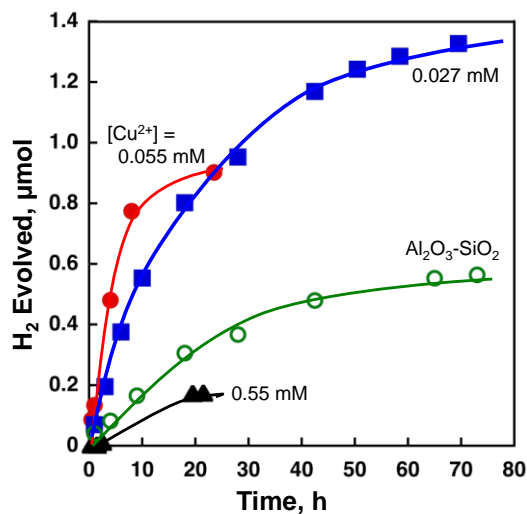


**Fig. 10.** Time courses of H<sub>2</sub> evolution under photoirradiation ( $\lambda > 340$  nm) of a deaerated phthalate buffer (pH 4.5) containing QuPh<sup>+</sup>-NA@sAlMCM-41 (5.0 mg, [QuPh<sup>+</sup>-NA] = 0.22 mM) and (COONa)<sub>2</sub> (50 mM) with Cu(NO<sub>3</sub>)<sub>2</sub> [0.55mM (black triangle), 0.055mM (red circle) or 0.027mM (blue square)] and QuPh<sup>+</sup>-NA@Al<sub>2</sub>O<sub>3</sub>-SiO<sub>2</sub> (7.1 mg, [QuPh<sup>+</sup>-NA] = 0.22 mM) and (COONa)<sub>2</sub> (50 mM) with Cu(NO<sub>3</sub>)<sub>2</sub> (0.055 mM) (green open circle).

evolution was observed for the reaction suspension containing QuPh<sup>+</sup>-NA@sAlMCM-41 and Cu ion in the concentration of 0.055 mM, however, the total amount of evolved H<sub>2</sub> was smaller than 1.0 μmol. More than 1.3 μmol H<sub>2</sub> was obtained from the reaction suspension containing Cu ion in the concentration of 0.027 mM although the H<sub>2</sub>-evolution rate was moderate (0.06 μmol h<sup>-1</sup>). When the concentration of Cu ion was increased to 0.55 mM, the total amount of evolved H<sub>2</sub> decreased to less than 0.2 μmol with slow H<sub>2</sub> evolution. The deceleration tendency observed for Cu ion is similar to that observed for the composite catalysts prepared with PtCl<sub>6</sub><sup>2-</sup> as shown in Fig. 1. At high concentrations, metal particles probably grew too many or too large to form an efficient composite catalyst in the mesopores of the mesoporous alumina-silica (sAlMCM-41). When the concentration of Cu(NO<sub>3</sub>)<sub>2</sub> was 0.055 mM, nanoparticles with a suitable number and size for H<sub>2</sub> evolution formed at first, and then, grew too many or too large. Size dependence of nanoparticles on photocatalytic H<sub>2</sub> evolution has been also reported for Ru nanoparticles without

a support [36]. Similarly, higher catalytic activity was obtained at lower concentrations of a  $\text{Ni}^{2+}$  precursor in the reaction suspensions as shown in Fig. S1.

Alumina-silica supports with non-porous structures are beneficial for improving reactivity of the composite catalysts loading Pt in terms of the  $\text{H}_2$  yield (vide supra). Thus, a composite catalyst with alumina-silica with a non-porous structure ( $\text{Al}_2\text{O}_3\text{-SiO}_2$ ) was prepared by photoirradiation of an aqueous buffer containing  $\text{QuPh}^+\text{-NA@Al}_2\text{O}_3\text{-SiO}_2$ ,  $\text{Cu}(\text{NO}_3)_2$  and oxalate. On the contrary to the composite catalysts loading Pt, non-porous  $\text{Al}_2\text{O}_3\text{-SiO}_2$  loading Cu exhibited low catalytic activity in terms of the  $\text{H}_2$ -evolution rate and  $\text{H}_2$  yield (Fig. 10, green open circle). Although Cu particles were not clearly observed by conventional TEM measurements, Cu particles may grow too large more than suitable size for  $\text{H}_2$  evolution at the lower surface area support due to its easy agglomeration properties.

The effects of precursors for Cu nanoparticles were examined on the photocatalytic  $\text{H}_2$  evolution, because composite catalysts prepared in an aqueous buffer containing Pt precursors exhibited large difference in catalytic activity depending on the electric charge of precursors (vide supra).  $\text{Cu}(\text{NO}_3)_2$  and  $\text{K}_2\text{CuCl}_4$  were employed as cationic and anionic precursors for preparing composite catalysts, respectively. However, no significant difference was observed for these two reaction systems (Fig. 11a). Similar catalytic activity obtained for the reaction systems employing  $\text{Cu}(\text{NO}_3)_2$  and  $\text{K}_2\text{CuCl}_4$  was ascribed to the labile property of the Cu precursors. The addition of oxalate to the solution containing  $\text{K}_2\text{CuCl}_4$  induced the shift of UV-vis absorption maxima from 750 to 700 nm, indicating that oxalate coordinate to  $\text{Cu}^{2+}$  ion of  $\text{K}_2\text{CuCl}_4$  to form an oxalate complex (Fig. 11b). The same absorption maxima in UV-vis spectrum observed for a buffer containing  $\text{Cu}(\text{NO}_3)_2$  and oxalic acid suggests that the structure of Cu species formed in the reaction solution is identical to that of  $\text{K}_2\text{CuCl}_4$  and oxalic acid in the reaction suspension

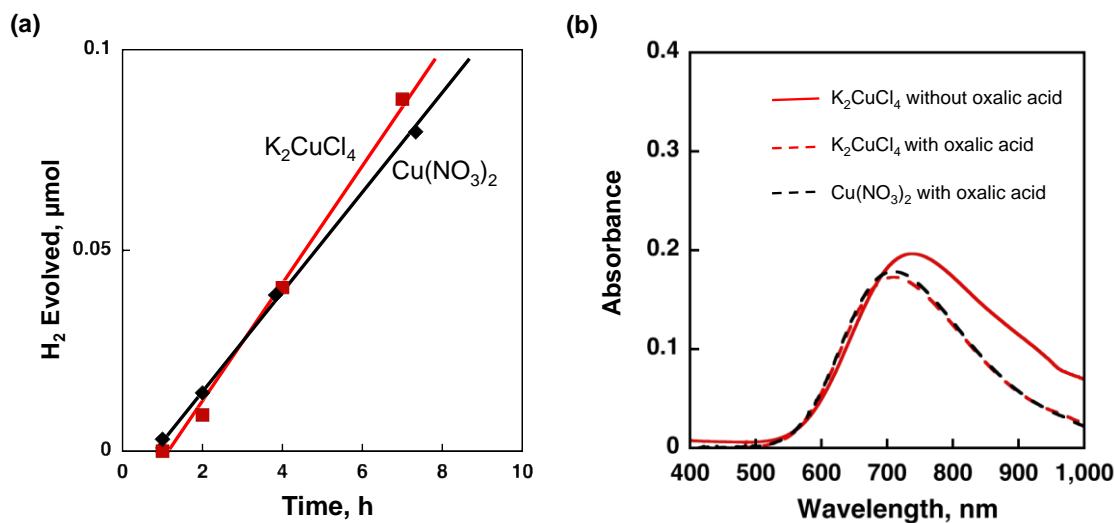


**Fig. 11.** (a) Time courses of H<sub>2</sub> evolution under photoirradiation ( $\lambda > 340$  nm) of a deaerated phthalate buffer (pH 4.5) containing QuPh<sup>+</sup>-NA@Al<sub>2</sub>O<sub>3</sub>-SiO<sub>2</sub> (7.1 mg, [QuPh<sup>+</sup>-NA] = 0.22 mM) and (COONa)<sub>2</sub> (50 mM) with Cu(NO<sub>3</sub>)<sub>2</sub> (black) or K<sub>2</sub>CuCl<sub>4</sub> (red) (0.055 mM). (b) UV-vis spectral change by addition of oxalic acid to a phthalate buffer containing Cu(NO<sub>3</sub>)<sub>2</sub> (black) or K<sub>2</sub>CuCl<sub>4</sub> (red). The solid line was obtained for the solution in the absence of oxalic acid and the dashed lines in the presence of oxalic acid.

before photoirradiation. Catalysis measurements of the reaction systems using a precursor for Cu particles selected from Cu(CF<sub>3</sub>SO<sub>3</sub>)<sub>2</sub>, Cu(ClO<sub>4</sub>)<sub>2</sub>, K<sub>2</sub>CuCl<sub>4</sub>, Cu<sub>2</sub>(OAc)<sub>4</sub>(H<sub>2</sub>O)<sub>2</sub>, [Cu(bpy)<sub>2</sub>]<sup>2+</sup> and [Cu(MeObpy)<sub>2</sub>]<sup>2+</sup> also manifested that the catalytic activity of the composite catalysts is independent of precursors (Fig. S2).

#### 4. Conclusion

Composite catalysts for photocatalytic H<sub>2</sub> evolution were prepared by *in situ* reduction of a Pt complex by utilizing the photocatalysis of QuPh<sup>+</sup>-NA supported on the surfaces of alumina-silica. The *in-situ* reduction allows to accommodate Pt nanoparticles close to QuPh<sup>+</sup>-NA on the support surfaces. For efficient H<sub>2</sub> evolution, selection of the precursor is important because positively charged precursors interact with negatively charged alumina-silica surfaces rather than

positively charged QuPh<sup>+</sup>-NA. Additionally, the suitable choices of the precursor concentration and morphology of a support are important to achieve high catalytic activity. By employing *in situ*-reduction procedure, Cu particles have been proved to act as an H<sub>2</sub>-evolution catalyst. However, no significant dependence of precursors on photocatalytic H<sub>2</sub> evolution because oxalate, which was used as an electron donor, readily form a kinetically rather stable complex with Cu ion. The finding disclosed here is beneficial to achieve highly active composite catalysts developed for artificial photosynthesis on a metal oxide support.

### **Acknowledgements**

This work was supported by JSPS KAKENHI (Nos. 24350069 and 15K14223 to Y.Y.) for Scientific Research from Japan Society for the Promotion of Science (JSPS). We sincerely acknowledge the Research Center for Ultra-Precision Science & Technology, Osaka University for TEM measurements.

### **Appendix A. Supplementary content**

Supplementary contents associated with this article can be found, in the online version, at <http://dx.doi.org/10.1016/j.cattod.XXXXX>.

### **References**

- [1] H. B. Gray, H. B., Nat. Chem. 1 (2009) 7.
- [2] D. Gust, T. A. Moore, A. L. Moore, Acc. Chem. Res. 42 (2009) 1890-1898.
- [3] D. G. Nocera, Acc. Chem. Res. 45 (2012) 767-776.
- [4] J. M. Thomas, Energy Environ. Sci. 7 (2014) 19-20.
- [5] T. A. Faunce, W. Lubitz, A. W. Rutherford, D. MacFarlane, G. F. Moore, P. Yang, D. G. Nocera, T. A. Moore, D. H. Gregory, S. Fukuzumi, K. B. Yoon, F. A. Armstrong, M. R. Wasielewski, S. Styring, Energy Environ. Sci. 6 (2013) 695.
- [6] A. Fujishima, K. Honda, Nature 238 (1972) 37.
- [7] A. Fujishima, X. Zhang, D. A. Tryk, Int. J. Hydrogen Energy 32 (2007) 2664-2672.
- [8] F. E. Osterloh, Chem. Soc. Rev. 42 (2013) 2294-2320.
- [9] A. Kudo, Y. Miseki, Chem. Soc. Rev. 38 (2009) 253-278.
- [10] T. Hisatomi, J. Kubota, K. Domen, Chem. Soc. Rev. 3 (2014) 1486-1503.

- [11] K. Maeda, K. Teramura, D. Lu, T. Takata, N. Saito, Y. Inoue, K. Domen, *Nature* 440 (2006) 295.
- [12] L. Z. Wu, B. Chen, Z. J. Li, C. H. Tung, *Acc. Chem. Res.* 47 (2014) 2177-2185.
- [13] S. Berardi, S. Drouet, L. Francàs, C. Gimbert-Suriñach, M. Guttentag, C. Richmond, T. Stolla, A. Llobet, *Chem. Soc. Rev.* 43 (2014) 7501-7519.
- [14] M. D. Kärkäs, E. V. Johnston, O. Verho, B. Åkermark, *Acc. Chem. Res.* 47 (2014) 100-111.
- [15] Z. Han, R. Eisenberg, *Acc. Chem. Res.* 47 (2014) 2537-2544.
- [16] H. Ozawa, K. Sakai, *Chem. Commun.* 47 (2011) 2227-2242.
- [17] S. Fukuzumi, Y. Yamada, T. Suenobu, K. Ohkubo, H. Kotani, *Energy Environ. Sci.* 4 (2011) 2754-2766.
- [18] M. Wang, Y. Na, M. Gorlov, L. Sun, *Dalton Trans.* (2009) 6458-6467.
- [19] S. Fukuzumi, *Eur. J. Inorg. Chem.* (2008) 1351-1362.
- [20] A. J. Esswein, D. G. Nocera, *Chem. Rev.* 107 (2007) 4022-4047.
- [21] J. Kiwi, M. Gratzel, *Nature* 281 (1979) 657-658.
- [22] K. Kalyanasundaram, J. Kiwi, M. Grätzel, *Helv. Chim. Acta* 61 (1978) 2720-2730.
- [23] J. M. Lehn, J. P. Sauvage, *New J. Chem.* 1 (1977) 449-451.
- [24] M. D. Kärkäs, O. Verho, E. V. Johnston, B. Åkermark, *Artificial Photosynthesis: Molecular Systems for Catalytic Water Oxidation. Chem. Rev.* 114 (2014) 11863-12001.
- [25] A. R. Parent, K. Sakai, *ChemSusChem* 7 (2014) 2070-2080.
- [26] S. Fukuzumi, D. Hong, *Eur. J. Inorg. Chem.* (2014) 645-659.
- [27] X. Sala, S. Maji, R. Bofill, J. Garia-Anton, L. S. Escriche, A. Llobet, *Acc. Chem. Res.* 47 (2014) 504-516.
- [28] S. Fukuzumi, Y. Yamada, *J. Mater. Chem.* 22 (2012) 24284-24296.
- [29] T. R. Cook, D. K. Dogutan, S. Y. Reece, Y. Surendranath, T. S. Teets, D. G. Nocera, *Chem. Rev.* 110 (2010) 6474-6502.
- [30] S. Fukuzumi, D. Hong, Y. Yamada, *J. Phys. Chem. Lett.* 4 (2013) 3458-3467.
- [31] S. Fukuzumi, Y. Yamada, *ChemSusChem* 6 (2013) 1834-1847.
- [32] J. Dasgupta, G. M. Ananyev, G. C. Dismukes, *Coord. Chem. Rev.* 252 (2008) 347-360.
- [33] J. H. Alstrum-Acevedo, M. K. Brennaman, T. J. Meyer, *Inorg. Chem.* 44 (2005) 6802-6827.
- [34] Y. Yamada, H. Tadokoro, S. Fukuzumi, *RSC Adv.* 3 (2013) 25677-25680.
- [35] H. Kotani, K. Ohkubo, S. Fukuzumi, *Faraday Discuss.* 155 (2012) 89-102.
- [36] Y. Yamada, T. Miyahigashi, H. Kotani, K. Ohkubo, S. Fukuzumi, *J. Am. Chem. Soc.* 133 (2011) 16136-16145.
- [37] Y. Yamada, T. Miyahigashi, K. Ohkubo, S. Fukuzumi, *Phys. Chem. Chem. Phys.* 14 (2012) 10564-10571.
- [38] Y. Yamada, T. Miyahigashi, H. Kotani, K. Ohkubo, S. Fukuzumi, *Energy Environ. Sci.* 5 (2012) 6111-6118.
- [39] Y. Yamada, S. Shikano, S. Fukuzumi, *J. Phys. Chem. C* 117 (2013) 13143-13152.
- [40] Y. Yamada, S. Shikano, S. Fukuzumi, *RSC Adv.* 5 (2015) 44912-44919.
- [41] Y. Yamada, A. Nomura, H. Tadokoro, S. Fukuzumi, *Catal. Sci. Technol.* 5 (2015) 428-437.
- [42] Y. Yamada, S. Shikano, T. Akita, S. Fukuzumi, *Catal. Sci. Technol.* 5 (2015) 979-988.
- [43] K. Sakai, Y. Kizaki, T. Tsubomura, K. Matsumoto, *J. Mol. Catal.* 79 (1993) 141-152.

- [44] R. C. Weast, in *Handbook of Chemistry and Physics*, CRC, Cleaveland, OH, 56th ed., 1975–1976.
- [45] K. S. W. Sing, D. H. Everett, R. A. W. Haul, L. Moscou, R. A. Pierotti, J. Rouquerol, T. Siemieniewska, *Pure Appl. Chem.* 57 (1985) 603-619.
- [46] H. Kotani, R. Hanazaki, K. Ohkubo, Y. Yamada, S. Fukuzumi, *Chem. Eur. J.* 17 (2011) 2777-2785.